Heighten Science PUBLICATIONS Corporation

ISSN
2640-2793

Research Article

Expression of C-type Natriuretic Peptide and its Specific Guanylyl Cyclase-Coupled Receptor in Pig Ovarian Granulosa Cells

Soo Mi Kim[1], Suhn Hee Kim[1], Kyung Woo Cho[1], Sun Young Kim[1] and Sung Zoo Kim[2]*

[1]Department of Physiology and Institute for Medical Sciences, Chonbuk National University Medical School, Jeonju 54907, Republic of Korea

[2]Department of Physiology, Chonbuk National University Medical School, Gungiro 20, Jeonju 54907, Republic of Korea

***Address for Correspondence:** Sung Zoo Kim, Ph.D, Department of Physiology, Chonbuk National University Medical School, Gungiro 20, Jeonju 54907, Republic of Korea, Tel: +82-63-270-3093; Fax: + 82-63-274-9892; Email: szkim@jbnu.ac.kr

Submitted: 08 August 2018
Approved: 21 August 2018
Published: 22 August 2018

Keywords: Natriuretic peptide receptor; Autoradiography; RT-PCR; Granulosa layer; Pig ovary; C-Type natriuretic peptide; Particulate guanylyl cyclase; Cgmp

Abstract

Background: C-type natriuretic peptide (CNP) was isolated from porcine brain and is a 22-amino acid peptide which belongs to the natriuretic peptide (NP) family. Even though this peptide shares structural similarity to other endogenous NPs including atrial natriuretic peptide (ANP) and brain natriuretic peptide (BNP) its receptor selectivity is different from other NPs. The present study was undertaken to investigate the expression of C-type natriuretic peptide (CNP) and its specific guanylyl cyclase (GC)-coupled receptor in the granulosa cells of the pig ovarian follicle.

Results: Specific ^{125}I-[Tyr^{0}]-CNP$_{(1-22)}$ binding sites were localized in the granulosa cell layer of the ovarian follicle with an apparent dissociation constant (K_d) and a maximal binding capacity (B_{max}) of 1.41±0.39 nM and 2.75±0.65 fmol/mm^2 respectively. Binding of ^{125}I-[Tyr^{0}]-CNP$_{(1-22)}$ to these sites was also prevented by atrial natriuretic peptide (ANP$_{(1-28)}$), brain natriuretic peptide (BNP$_{(1-26)}$) and des[Gln^{18},Ser^{19},Gly^{20}, Leu^{21},Gly^{22}] ANP$_{(4-23)}$ (C-ANP). Production of 3',5'-cyclic guanosine monophosphate (cGMP) by particulate GC in the granulosa cell membranes was stimulated by natriuretic peptides (NPs) with a rank order of potency of CNP$_{(1-22)}$>>BNP$_{(1-26)}$>ANP$_{(1-28)}$. HS-142-1, a selective antagonist of the two recognized GC-coupled NPRs, inhibited CNP$_{(1-22)}$-stimulated cGMP production in granulosa cell membranes in a dose-dependent manner. Also mRNAs for all three recognized NPRs were detected in granulosa cells using reverse transcriptase-polymerase chain reaction (RT-PCR). Serial dilution curves of granulosa cell extracts were parallel to the standard curve of synthetic CNP.

Conclusion: These results indicate that CNP and its specific receptor are expressed in the granulosa cells of the pig ovary, and suggest that CNP may be a local autocrine and/or paracrine regulator via activation of its specific GC-coupled receptor, NPR-B.

Introduction

C-type natriuretic peptide (CNP) was isolated from porcine brain [1] and is a 22-amino acid peptide which belongs to the natriuretic peptide (NP) family. Even though this peptide shares structural similarity to other endogenous NPs including atrial natriuretic peptide (ANP) and brain natriuretic peptide (BNP) [1-3], its receptor selectivity is different from other NPs. The guanylyl cyclase (GC)-coupled NP receptor subtype A (NPR-A) is activated solely by ANP and BNP, and exerts well-defined biological functions via activation of particulate GC. On the other hand, the GC-coupled

How to cite this article: Kim SM, Kim SH, Cho KW, Kim SY, Kim SZ. Expression of C-type Natriuretic Peptide and its Specific Guanylyl Cyclase-Coupled Receptor in Pig Ovarian Granulosa Cells. Insights Clin Cell Immunol. 2018; 2: 014-025. https://dx.doi.org/10.29328/journal.icci.1001004

NP receptor subtype B (NPR-B) is selectively activated by CNP [4,5]. In contrast to ANP or BNP, which are circulating hormones, CNP is likely to be an autocrine or paracrine mediator because it was detectable only at very low levels in plasma [6]. Since NPR-B is relatively specific for CNP, the localization of NPR-B predicates the possible biological actions of CNP in target organs [7]. Although NPR-B is expressed widely in the vascular smooth muscle and induces smooth muscle relaxation [8], it is also expressed in neural tissues including fetal telencephalon and somites [9,10], hypothalamus [11] and pituitary gland [12], and in atrial myocytes [13]. In these tissues, it has been suggested that CNP may be involved in modulation of the embryonic growth, neural transmission, other hormone synthesis and/or secretion, and membrane Ca^{2+} channel activity [14,15]. Therefore, CNP system may serve autocrine and/or paracrine functions rather than the well-defined functions of ANP and BNP as circulating hormones.

Gonadotropins and the ovarian steroid hormones act together in the hypothalamic-pituitary-gonadal axis to regulate follicular development and oocyte maturation, but local mediators within the ovary may also control follicular development. As one example, the intra-ovarian renin-angiotensin system has been proposed to control follicular development [16]. Another possible factor may be atrial natriuretic peptide (ANP), which is a functional antagonist to angiotensin II (Ang II) in other tissues [17]. ANP occurs in the ovary [18,19]. The identification of mRNA encoding ANP and the immunohistochemical localization of ANP in the granulosa cells of the pig ovary suggests that ovarian granulosa cells elaborate ANP [20]. ANP has been shown to stimulate [21-24] or inhibit [25] the secretion of pregesterone in the ovary. Moreover, the presence of specific binding sites for ANP has been found in several ovarian tissues of mammals; in the preovulatory follicles of human [26], in cultured human granulosa-lutein cells [21], in the bovine corpus luteum [18] and in porcine granulosa and theca externa cells [27]. Furthermore, ANP specifically stimulates a particulate GC in bovine luteal cells [28]. In comparison to the intra-ovarian ANP system, the role of CNP in the ovaries remains to be studied. Recently, CNP has been identified in the rat ovary but its sites of action have not been elucidated [29]. The purpose of the present study was to define the intra-ovarian CNP system. We have identified a CNP-specific GC-coupled receptor and endogenous CNP synthesis, using quantitative in vitro autoradiography, activation of particulate GC by NPs, RT-PCR, radioimmunoassay (RIA). Thus, CNP and its receptor may mediate autocrine and/or paracrine effects in the ovary.

Materials and Methods

Collection and transportation of ovaries

For the separation of granulosa cells, ovaries from healthy young pigs were collected at a slaughterhouse within 10 min of slaughter, and immediately transported to the laboratory in a sterile container in ice-cold 0.9% NaCl solution. For in vitro receptor autoradiography, other ovaries were collected from pigs within 10 min of slaughter, and were immediately snap frozen in liquid nitrogen, and stored in sealed boxes at -70°C prior to frozen sectioning.

In vitro autoradiographic binding of ^{125}I-[Tyr^{0}]-CNP$_{(1-22)}$

Serial 20 µm sections were cut on a cryostat at -20°C, thaw-mounted onto gelatin-chrom-alum coated slides, and then dried in a desiccator at 4°C overnight before incubation. Incubation with ^{125}I-[Tyr^{0}]-CNP$_{(1-22)}$ (specific activity 1,700 Ci/mmol) was performed as previously reported [9,10]. Briefly, the sections were washed with 150 mM NaCl-0.5% acetic acid (pH 5.0) at room temperature for 10 min in order to remove endogenous NPs, and then preincubated with 30 mM phosphate buffer (pH 7.2) containing 120 mM NaCl and 1 mM phenanthroline at room temperature for 10 min. As shown in Figure 1, acidic washing increases the specific binding capacity for ^{125}I-[Tyr^{0}]-

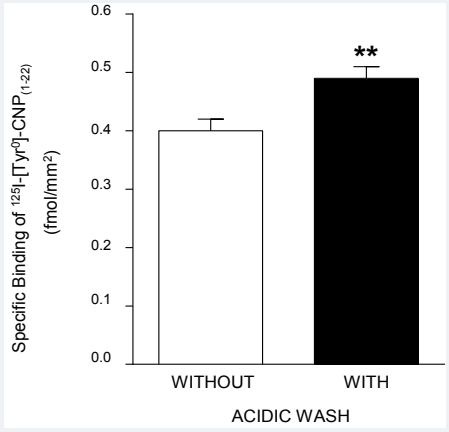

Figure 1: Effect of acidic washing on maximal specific binding capacities of ^{125}I-[Tyr^{0}]-CNP$_{(1-22)}$ in the granulosa cell layer of the pig ovary. Each bar represents means±SE of results from 20 follicles. **P<0.01 for differences of specific ^{125}I-[Tyr^{0}]-CNP$_{(1-22)}$ binding density between non-acidic washed and acidic washed ovarian sections of the pig.

CNP$_{(1-22)}$ in the granulosa cell layer of the pig ovary. The sections were incubated with ^{125}I-[Tyr^{0}]-CNP$_{(1-22)}$ in fresh preincubation buffer containing 40 µg/ml bacitracin, 100 µg/ml phenylmethylsulfonyl fluoride (PMSF), 10 µg/ml leupeptin, and 0.5% bovine serum albumin (BSA) at room temperature. After incubation, the sections were rinsed and washed with fresh preincubation buffer for 5 min at 4°C. Subsequently, they were rinsed three times in cold distilled water at 4°C and quickly dried under a stream of cold air. In preliminary experiments, the time course of the specific binding of the radioligand was established in the presence or absence of excess unlabeled CNP$_{(1-22)}$. The saturable specific binding of ^{125}I-[Tyr^{0}]-CNP$_{(1-22)}$ was assessed in serial sections which were incubated with increasing concentrations (0-750 pM) of the radioligand in the presence or absence of 1 µM CNP$_{(1-22)}$. Competitive inhibition of the binding of ^{125}I-[Tyr^{0}]-CNP$_{(1-22)}$ was examined in consecutive sections by coincubating with various concentrations of unlabeled CNP$_{(1-22)}$, ANP$_{(1-28)}$, BNP$_{(1-26)}$ or des[Gln^{18}, Ser^{19}, Gly^{20}, Leu^{21}, Gly^{22}] ANP$_{(4-23)}$ (C-ANP). To test the specificity of ^{125}I-[Tyr^{0}]-CNP$_{(1-22)}$ binding, adjacent sections were incubated in the presence of the unrelated peptides, angiotensin II or arginine vasopressin (all 10 µM).

Computerized microdensitometry of autoradiograms

Autoradiographic images were generated by exposing sections to Hyperfilm-^{3}H (Amersham International plc, Buckinghamshire, U.K.) in X-ray cassettes together with 20 µm-thick ^{125}I-labeled polymer standard strips (Amersham International plc) at room temperature for 7 days. Autoradiograms were developed in Kodak D-19 developer (Eastman Kodak Co, Rochester, NY) for 3 min and fixed in Kodak rapid fixer for 5 min at room temperature. Sections were then fixed in formaldehyde and stained with hematoxylin and eosin [9,10].

Autoradiographic images were viewed with a Leica Wild M420 Macroscope, and captured using a Sony video camera with CCD iris and a Hamamatsu AC adaptor connected to a Power Macintosh 8100/80AV computer. Regional binding of ^{125}I-[Tyr^{0}]-CNP$_{(1-22)}$ in the ovary was analysed using the PRISM image program (Version 3.6-1, Improve Vision, Coventry, UK). Optical densities were measured as disintegrations per minute (dpm) per square millimeter, based on the comparison with the calibration curve derived from the autoradiograms of the ^{125}I standard microscales included in

each X-ray cassette. These data were converted into femtomoles ^{125}I-[Tyr^{0}]-CNP$_{(1-22)}$ bound per square millimeter, as described elsewhere [30]. The number of ligand binding sites of different affinities, their apparent dissociation constants (K_d) and inhibitory constants (K_i), and their maximal binding capacities (B_{max}) on particular structures were derived separately in each individual using the LIGAND iterative model-fitting computer program [31].

Particulate GC activity of granulosa cells

Granulosa cells were homogenized at 4°C in 30 mM phosphate buffer (pH 7.2) containing 120 mM sodium chloride and 1 mM phenanthroline by three 30-second bursts of 27,000 rpm using a Polytron homogenizer (Brinkmann Instruments, Westbury, NY). The homogenate was centrifuged at 1,500xg for 10 min at 4°C, and the supernatant was recentrifuged at 40,000xg for 60 min at 4°C. The membrane pellet was washed three times with 50 mM Tris-HCl (pH 7.4) and resuspended in this solution. Protein contents were determined by a bicinchoninic acid assay kit (Sigma Chemical Co, St. Louis, MO). Particulate GC activity was measured according to the method described elsewhere [9]. Aliquots of 10 µg of membrane protein of the suspension were incubated for 15 min at 37°C in a final volume of 125 µl of 50 mM Tris-HCl (pH 7.6) containing 1 mM isobutylmethylxanthine, 1 mM guanosine triphosphate, 0.5 mM adenosine triphosphate, 15 mM creatine phosphate, 80 µg/ml creatine phosphokinase, and 4 mM magnesium chloride, plus a range of concentrations of either CNP$_{(1-22)}$, BNP$_{(1-26)}$, or ANP$_{(1-28)}$. To test the specificity of GC-coupled NPR, aliquots were also incubated 1 µM CNP$_{(1-22)}$ plus HS-142-1 (0 to 1,000 µg/ml) [31,32]. Incubations were stopped by adding 375 µl of ice cold 50 mM sodium acetate (pH 5.8) and boiling for 5 min. Samples were then centrifuged at 10,000xg for 5 min at 4°C.

Production of cGMP was measured in the supernatants by equilibrated radioimmunoassay (RIA). In brief, standards or samples were taken up in a final volume of 100 µl of 50 mM sodium acetate buffer (pH 4.8), and then 100 µl of diluted cGMP antiserum (Calbiochem-Novabiochem Co, San Diego, CA) and iodinated cGMP (10,000 cpm/100 µl, Specific activity=2,200 Ci/mmole, Du Pont-New England Nuclear, Wilmington, DE) were added and incubated for 24 hr at 4°C. The bound form was separated from the free form by charcoal suspension. RIA for cGMP was done on the day of experiments, and all samples in an experiment were analyzed in a single assay. Nonspecific binding was <2.5%. The 50% intercept was at 0.39±0.03 pmol/tube (n=15). The intra and interassay coefficients of variation were 6.7 (n=12) and 8.6% (n=9), respectively. Average results of determinations were expressed as picomoles of cGMP generated per milligram protein per minute.

Iodination of CNP$_{(1-22)}$

Iodinated CNP$_{(1-22)}$ was prepared as described for ANP [32]. In brief, 5 µg of synthetic [Tyr^{0}]-CNP$_{(1-22)}$ (Peninsula Laboratories, Belmont, CA) was introduced into a vial containing 25 µl of 0.5 M phosphate buffered saline (pH 7.4) followed by an addition of 1 mCi of ^{125}I-Na (Amersham International plc). Chloramine-T (10 µg/10 µl) was added to the reaction vial, mixed gently, and 30 sec later the reaction was terminated by BSA solution (60 mg/200 µl). The reaction mixture was immediately applied to a Sephadex G-25 column (1x24 cm) and was eluted with 0.1 M acetic acid containing 0.3% BSA, 0.3% lysozyme, 0.1% glycine, and 200 kallikrein inhibitor unit/ml aprotinin. The iodinated [Tyr^{0}]-CNP$_{(1-22)}$ was divided and stored at -70°C until used. Immediately before using, ^{125}I-[Tyr^{0}]-CNP$_{(1-22)}$ was repurified by high performance liquid chromatography (HPLC)

on a reverse phase μBondapak column (Waters Associates, Milford, MA) with a linear gradient (20% to 60% acetonitrile) elution. The specific activity of ^{125}I-[Tyr^{0}]-CNP$_{(1-22)}$, measured by RIA technique [33] was approximately 1,700 Ci/mmol. For the RIA of CNP$_{(1-22)}$, antibody was obtained from Peninsula Laboratories.

RT-PCR of CNP mRNA

Total RNA was extracted from the granulosa cells using TRI reagent (MRC, Cincinnati, OH) according to the manufacturer's protocol. Total RNA concentrations were quantitated by UV spectrophotometry. Five hundred nanograms of total RNA were suspended in 20 μl buffer containing 10 mM Tris (pH 8.3); 50 mM KCl; 5 mM $MgCl_2$; 1 mM each of deoxy (d)-ATP, dCTP, dGTP, and dTTP; 20 U ribonuclease inhibitor; 2.5 μM random hexamers; and 150 U Moloney leukemia virus reverse transcriptase (Perkin Elmer, Branchburg, NJ) and reverse transcribed at room temperature for 10 min and 42°C for 30 min. The reaction was stopped by heat inactivation for 5 min at 99°C and then chilled on ice. Complementary DNA products were amplified by PCR with sense 5′-CTCTCCCAGCTGATCGCCTG-3′ (7-26) and antisense 5′-TAACATCCCAGACCGCTCAT-3′ (361-380) primers [2]. Fifty microliters of PCR buffer contained 10 mM Tris (pH 8.3); 50 mM KCl; 2 mM $MgCl_2$; 200 μM each of dATP, dCTP, dGTP, and dTTP; 2.5 U Taq polymerase; and 50 pM each of sense and antisense primers. The temperature profile of amplification consisted of 30 sec denaturation at 95°C, 1 min annealing at 64°C, and 2 min extension at 72°C for 50 cycles. PCR products were separated in 2% agarose gels, and bands were visualized by ethidium bromide staining. Photographs of gels were taken with Polaroid 665 film.

RT-PCR of NPR mRNAs for subtypes: One microgram of total RNA was reverse transcribed the same method as described above. Complementary DNA products were amplified by PCR using the following primers [4,34]:

NPR-A sense, 5′-AAGAGCCTGATAATACCTGAGTACT-3′;

NPR-A antisense, 5′-TTGCAGGCTGGGTCCTCATTGTCA-3′;

NPR-B sense, 5′-AACGGGCGCATTGTGTATATCTGCGGC-3′;

NPR-B antisense, 5′-TTATCACAGGATGGGTCGTCCAAGTCA-3′;

NPR-C sense, 5′-GTCCTGCAGTTACGTGAAGTACTCAGAGCTGG-3′;

NPR-C antisense, 5′-CCGAATTCATCACCAATAACCTCCTGGG-3′.

Fifty microliters of PCR buffer contained 10 mM Tris (pH 8.3); 50 mM KCl; 2 mM $MgCl_2$; 200 μM each of dATP, dCTP, dGTP, and dTTP; 2.5 U Taq polymerase; and 100 pmol each of sense and antisense primers. A hot start PCR was used to increase the specificity of amplification. The temperature profile of amplification consisted of 30 sec denaturation at 95°C, 1 min annealing at 60°C for NPR-A and NPR-B, and 64°C for NPR-C and 2 min extension at 72°C for 40-50 cycles. PCR products were separated in 1.4% agarose gels and bands were visualized by ethidium bromide staining. Photographs of gels were taken with Polaroid 665 film. PCR products were confirmed by sequence analysis (data not shown).

Statistical analysis

The figures show the results (means±SE values) of individual experiments involving three or more replicates. These are representative of results obtained in at least three similar experiments or show data from multiple experiments pooled as described in the figure legends. Comparisons of results were performed by paired Student's t-test and ANOVA with Duncan multiple range test, accepting $P<0.05$ as the criterion of significance.

Results

Autoradiographic Localization of ^{125}I-[Tyr^{0}]-CNP$_{(1-22)}$ Bindings:

As shown in Figure 2A, the binding of ^{125}I-[Tyr^{0}]-CNP$_{(1-22)}$ was localized in ovarian follicles of a wide range of sizes. The densest binding of ^{125}I-[Tyr^{0}]-CNP$_{(1-22)}$ occurred in the granulosa layer of the follicles. A low density of binding sites was observed in the theca externa layer of the follicles, but not in the theca interna layer and the interstitial region of the ovary (Figure 2C). In the presence of 1 μM unlabeled CNP$_{(1-22)}$, binding to the granulosa and theca externa layers of follicles was completely displaced, but the diffuse background binding was not affected (Figure 2B). Nonspecific binding was 0.59±0.05% of total binding in these structures. Ten micromolar unrelated peptides including angiotensin II or arginine vasopressin did not displace the binding of ^{125}I-[Tyr^{0}]-CNP$_{(1-22)}$ to either granulosa or theca externa (data not shown). Two hundred and fifty picomolar ^{125}I-[Tyr^{0}]-CNP$_{(1-22)}$ bound specifically to granulosa cell layer, and reached equilibrium at 40 min at room temperature (data not shown).

The displacement of ^{125}I-[Tyr^{0}]-CNP$_{(1-22)}$ binding to granulosa by heterologous ligands was also investigated (Figure 3). Unlabeled 10 μM ANP$_{(1-28)}$ and BNP$_{(1-26)}$, as more selective endogenous ligands for NPR-A, respectively inhibited 99.50±0.15 and 99.750.05% of the specific binding of ^{125}I-[Tyr^{0}]-CNP$_{(1-22)}$ to the granulosa. In the presence of 10 μM unlabeled C-ANP, a specific ligand for NPR-C, the specific binding to the granulosa was inhibited by 93.22±1.61%.

Competitive Inhibition of Autoradiographic ^{125}I-[Tyr^{0}]-CNP$_{(1-22)}$ Bindings:

Analysis of the competitive inhibition of the binding of ^{125}I-[Tyr^{0}]-CNP$_{(1-22)}$ to the granulosa layers in preovulatory follicles by increasing concentrations of unlabeled CNP$_{(1-22)}$ was consistent with a single high affinity binding site for ^{125}I-[Tyr^{0}]-CNP$_{(1-22)}$ (Figure 4A). In the follicles, ^{125}I-[Tyr^{0}]-CNP$_{(1-22)}$ bound reversibly to granulosa with a K_d and B_{max} of 1.41±0.39 nM and 2.750.05 fmol/mm^2 (Table 1). Increasing concentrations of ANP$_{(1-28)}$, BNP$_{(1-26)}$ and C-ANP also progressively inhibited the specific binding of ^{125}I-[Tyr^{0}]-CNP$_{(1-22)}$ to granulosa (Figure 4B). The effects were consistent with sites of a single affinity for ANP$_{(1-28)}$, BNP$_{(1-26)}$, and C-ANP (Table 1). C-ANP competed with much less affinity than any of the other ligands, including CNP$_{(1-22)}$, for the binding sites of ^{125}I-[Tyr^{0}]-CNP$_{(1-22)}$ on the granulosa cell layer ($p<0.01$), but B_{max} values have not significantly different among the unlabeled ligands (Table 1).

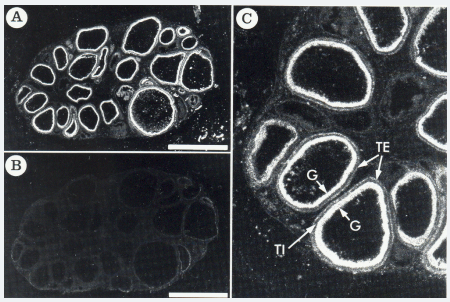

Figure 2: Dark-field photomicrograph of autoradiograms of the pig ovarian sections incubated in the presence of 250pM ^{125}I-[Tyr^{0}]-CNP$_{(1-22)}$ (A) and its adjacent section incubated in 250pM ^{125}I-[Tyr^{0}]-CNP$_{(1-22)}$ plus 1 μM unlabeled CNP$_{(1-22)}$ (B). ^{125}I-[Tyr^{0}]-CNP$_{(1-22)}$ binding sites appear as white silver grains. As shown in C with more high magnification of A in part, specific ^{125}I-[Tyr^{0}]-CNP$_{(1-22)}$ binding sites were localized in the granulosa (G) and the theca externa (TE) layers of the follicles, but none in the theca interna (TI) layer. Bars=5mm.

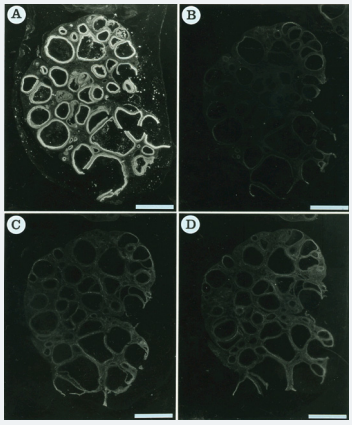

Figure 3: Dark-field photomicrograph of autoradiograms of the pig ovarian sections incubated in the presence of 250pM ^{125}I-[Tyr^{0}]-CNP$_{(1-22)}$ (A) and its adjacent sections incubated in 250 pM ^{125}I-[Tyr^{0}]-CNP$_{(1-22)}$ plus 10 μM unlabeled ANP$_{(1-28)}$ (B), 10 μM unlabeled BNP$_{(1-26)}$ (C) or 10 μM unlabeled C-ANP (D). ^{125}I-[Tyr^{0}]-CNP$_{(1-22)}$ binding sites appear as white silver grains. Bars=5 mm.

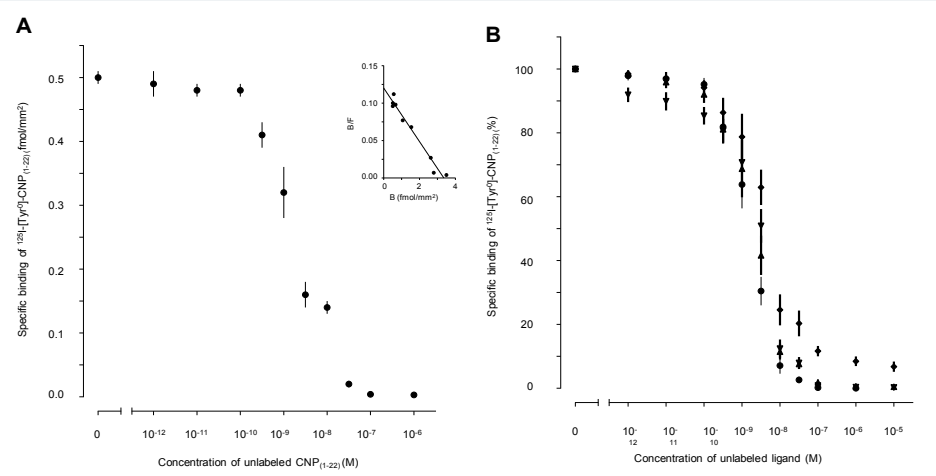

Figure 4: Competitive inhibition curves of specific ^{125}I-[Tyr^{0}]-CNP$_{(1-22)}$ bindings to frozen sections of the pig ovary. (A) Mean values from 10 individuals were plotted for the competition of binding of 250 pM ^{125}I-[Tyr^{0}]-CNP$_{(1-22)}$ to the granulosa cell layer by increasing concentrations of unlabeled CNP$_{(1-22)}$. Inset: representative Scatchard plot obtained from 1 individual of these pigs. B/F, bound/free. (B) Competitive inhibition of the maximal specific binding of 250 pM ^{125}I-[Tyr^{0}]-CNP$_{(1-22)}$ to the granulosa cell layer by increasing concentrations of unlabeled CNP$_{(1-22)}$ (•), ANP$_{(1-28)}$ (▲), BNP$_{(1-26)}$ (▼) or C-ANP (■).

Table 1: Mean values of binding constants for specifically reversible bindings of ^{125}I-[Tyr^{0}]-CNP$_{(1-22)}$ by unlabeled ligands in granulosa cell layer of the pig ovary.

Ligand	K_d (nM)	K_i (nM)	B_{max} (fmol/mm^2)
CNP$_{(1-22)}$	1.41±0.39		2.75±0.65
ANP$_{(1-28)}$		1.800.41	2.23±0.49
BNP$_{(1-26)}$		2.050.40	2.35±0.62
C-ANP		4.98±1.42*	2.64±0.68

Values are mean±S.E (n=10 ovaries). Apparent dissociation constants (K_d), inhibitory constants (K_i) and maximum binding capacities (B_{max}) were assessed from competitive inhibition of 250 pM ^{125}I-[Tyr^{0}]-CNP$_{(1-22)}$ binding by various concentrations of unlabeled ligands. *P<0.01 for comparison of corresponding mean values between affinities of CNP$_{(1-22)}$ and other ligands.

Particulate GC activity

The rate of cGMP production by particulate GC activation of granulosa cell membranes was basally 26.300.80 pmol/mg protein/min. As shown in Figure 5A, CNP$_{(1-22)}$, BNP$_{(1-26)}$ and ANP$_{(1-28)}$ each produced dose-dependent increases in cGMP production. At 1 μM

concentration, the rates of cGMP production by $CNP_{(1-22)}$, $BNP_{(1-26)}$ and $ANP_{(1-28)}$ were 77.13±3.36, 41.991.50 and 34.97±1.51 pmol/mg protein/min, respectively. $CNP_{(1-22)}$ caused the highest increment of cGMP production with half-maximal response (EC_{50}) of ~10 nM. The maximum increase in cGMP, measured in response to 1 µM $CNP_{(1-22)}$ was ~3 fold over basal levels. But the maximum cGMP production stimulated by $BNP_{(1-26)}$ or $ANP_{(1-28)}$ was less than that by $CNP_{(1-22)}$ ($p< 0.01$). HS-142-1, a selective antagonist for the GC-coupled NPR, inhibited $CNP_{(1-22)}$-stimulated cGMP production in a dose-dependent manner (Figure 5B). At a concentration of 1,000 µg/ml, HS-142-1 inhibited completely the $CNP_{(1-22)}$-stimulated cGMP production by the granulosa cell membranes.

Detection of NPR-B mRNA by RT-PCR

The presence of NPR-B transcripts was tested by RT-PCR. In granulosa cells, NPR-B cDNA was found in ethidium bromide stained gels with the expected size of 692 base pairs (bp) (Figure 6, lane 4) after 50 cycles of amplification, and NPR-A transcripts with 451 bp were also detected after 40 cycles of amplification (Figure 6, lane 2). RT-PCR data from the pituitary gland of rat, which express NPR-A and NPR-B transcripts [12], were also shown for comparison. NPR-C transcripts were also found (Figure 6). No transcripts were observed in RNA samples incubated without Moloney leukemia virus reverse transcriptase.

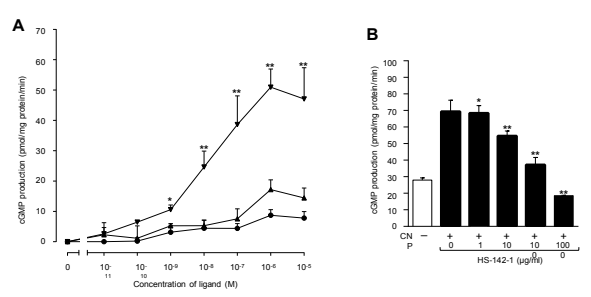

Figure 5: (A) Dose-dependent cGMP production in response to NPs in the granulosa cell membranes from similar size follicles of the pig ovary. Membranes were prepared by pooling of the granulosa cells from 20 individuals, and incubated in the presence of $CNP_{(1-22)}$ (●), $BNP_{(1-26)}$ (▲) and $ANP_{(1-28)}$ (■). Basal values (26.30±0.80 pmol/mg protein/min) obtained from the incubation in the absence of NPs were subtracted from each point. The data were expressed as mean ± SE of triplicate determinations. *P<0.05 and **P<0.01 for comparison of $CNP_{(1-22)}$-treated group vs. $BNP_{(1-26)}$ or $ANP_{(1-28)}$-treated groups. (B) Effect of HS-142-1 on $CNP_{(1-22)}$-stimulated cGMP production in the granulosa cell membranes of the pig ovary. Membranes were incubated with 1 µM $CNP_{(1-22)}$ either alone or in the presence of increasing concentrations of HS-142-1. The data were expressed as mean±SE of triplicate determinations. *P<0.05 and **P<0.01 for comparison of $CNP_{(1-22)}$ only-treated group vs. $CNP_{(1-22)}$ plus HS-142-1-treated groups.

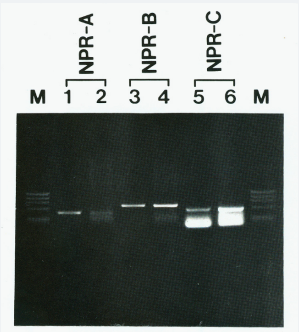

Figure 6: Detection of NPR transcripts by RT-PCR in the granulosa cell of the pig ovary (lanes 2, 4 and 6), and in the pituitary gland (lanes 1 and 3) and renal glomeruli (lane 5) of the rat for positive control. Bands representing the NPR-B subtype were detected in ethidium bromide-stained gels after 50 cycles of amplification in the ovarian granulosa cell extracts. Bands for NPR-A and NPR-C transcrips were also found in the granulosa cells. M, DNA molecular marker (174 RF DNA, *Hae* III cut).

Discussion

The new findings in our present study are the characteristics of CNP specific GC-coupled receptors and CNP in the pig ovarian granulosa cells, providing evidence for the presence of CNP system in these cells. Intra-ovarian NP systems have already generated considerable interest. The presence of ANP in ovarian extracts from cattle [18] and rats [19], the identification of mRNA encoding ANP [20], and the secretion [20] of ANP by granulosa cells of the pig ovary have all established the ovary as a site of synthesis and secretion of ANP. Furthermore, specific ANP binding sites have been detected in ovarian tissues [21-26]. Other studies have suggested that ovarian ANP might be involved in the regulation of follicular growth [19,20], steroidogenesis [21-25], and ovulation [35,36]. Nevertheless, the role of NPs within the ovary is not well understood. Recently, the presence of CNP and NPR-B have been detected in the whole rat ovary [29]. Rat ovarian CNP levels and the binding activity of the GC-coupled receptor vary with the estrous cycle, suggesting its possible role in follicular development and in the maturation or function of preovulatory follicles. However, it still has questions about the site of function and preference for NP within ovarian structures.

Our results clearly provide direct evidence for the local CNP system in the granulosa cells. Autoradiographic results revealed that specific binding sites of ^{125}I-[Tyr^{0}]-CNP$_{(1-22)}$ were localized in the granulosa and theca externa cell layers of primary and maturing follicles, but binding was not observed in the theca interna layer or in the interstitial region of the ovary. Ovarian tissue sections were washed by an acidic solution before incubation with ^{125}I-[Tyr^{0}]-CNP$_{(1-22)}$ to remove any unmeasured endogenous NP occupying receptors. This acidic washing significantly increased the maximal specific ^{125}I-[Tyr^{0}]-CNP$_{(1-22)}$ binding densities of the granulosa cell layer by about 17%. This suggests that the NPRs in granulosa cells are indeed exposed to endogenous NPs.

Classically, the receptors for NPs have been classified as biological and clearance receptors. The biological receptors consist of two subtypes, designated NPR-A and NPR-B, with two monomeric proteins of molecular mass of 120-140 kDa containing an extracellular ligand-binding domain and an intracellular guanylate cyclase (GC) catalytic domain [4,5]. Moreover, the biological receptor subtypes have been characterized by their ligand selectivity with the rank order of potency for cGMP production; relative potencies for NPR-A and NPR-B are ANP>BNP>>CNP and CNP>>BNP>ANP, respectively [4,5,8]. Therefore, the predominant ligands for NPR-A are ANP and BNP, whereas NPR-B binds selectively to CNP. The clearance receptor, NPR-C, consists of a single cloned protein which is a disulfide-linked 60-70 kDa homodimer without an intracelluar GC catalytic domain [37]. This subtype is a unique protein that binds all of NPs including C-ANP, a synthetic peptide which does not bind to either NPR-A or NPR-B [37-40].

Since specific binding with ^{125}I-[Tyr^{0}]-CNP$_{(1-22)}$, which is a selective ligand for NPR-B subtype rather than NPR-A [41], was displaced by ANP$_{(1-28)}$, BNP$_{(1-26)}$ and C-ANP, it seems likely that NPR-B in the granulosa cells either does not bind the radioligand efficiently or is too low to be detected by in vitro autoradiographic technique. As shown in Figure 6, RT-PCR products for NPRs clearly demonstrate that the transcripts for NPR-B as well as NPR-A and NPR-C are all present in the granulosa cells. We found that an excess concentration of C-ANP (10 μM) inhibited about 93% of the bindings of ^{125}I-[Tyr^{0}]-CNP$_{(1-22)}$ to its specific granulosa cell layer binding sites. In preliminary studies, we have found that specific bindings of ^{125}I-ANP$_{(1-28)}$ in these structures were also inhibited about 95% by 10 μM of C-ANP. This implies that a main population of total NPRs in this structure is NPR-C, and the remained binding sites are NPR-B and/or NPR-A.

Although it seems that NPR-C is proportionally a major population among NPRs in the pig ovarian granulosa cells by a quantitative in vitro autoradiographic analysis, the predominant localization of GC-coupled NPRs is necessary to understand the possible biological actions of NPs on these cells. As shown in Figure 5, cGMP accumulation by ovarian granulosa cell membranes was stimulated more strongly by CNP than ANP or BNP. To our knowledge, these results demonstrate for the first time the predominant localization of CNP-sensitive particulate GC in the intraovarian tissues. Furthermore, HS-142-1, a novel and non-peptide NPR antagonist isolated from Aureobasidium sp. [42], was able to inhibit the CNP-stimulated cGMP production in the pig ovarian granulosa cells in a dose-dependent manner. HS-142-1 competitively and selectively inhibits cGMP production via activation of GC-coupled NPR-B by CNP as well as NPR-A by ANP or BNP [42,43]. These results suggest that NPR-B is the predominant subtype of biological NPR expressed in the pig ovarian granulosa cells.

In summary, we provide evidence for the presence of all components of CNP system within the granulosa cells of the pig ovarian follicles. Our results suggest that the CNP produced by granulosa cells have roles through the cGMP accumulation via activation of GC-coupled NPR-B for intraovarian functions.

Acknowledgement

We are very grateful to Dr. John Brown, Physiological Laboratory, University of Cambridge, for critical comments for the experiment, and to Dr. S. Nakanishi, Tokyo Research Laboratories, Kyowa Hakko Kogyo Co. Ltd., Japan for generous gift of HS-142-1 used. We also thank technicians, Jeonju Regional Slaughterhouse of National Livestock Cooperative Federation, for their kind assistance for the ovary collection. The valuable technical assistance of Keum Nim Koh, Sook Jeong Lee and Kyung Sun Lee are grateful acknowledged. This work was supported by the Korea Science and Engineering Foundation (#95-0403-01-01-3), by the Research Fund of Korean Ministry of Education through Chonbuk National University Institute for Medical Sciences, Republic of Korea, and by grants from the Medical Research Center Program (grant no. NRF-2017R1A5A2015061 and 2018R1D1A1B07048569) through the National Research Foundation, which is funded by the Korean government (MSIP).

References

1. Sudoh T, Minamino N, Kangawa K, Matsuo H. C-type natriuretic peptide (CNP): a new member of natriuretic peptide family identified in porcine brain. Biochem Biophys Res Commun. 1990; 168: 863-870. **Ref.:** https://tinyurl.com/yc99nj4v

2. Kojima M, Minamino N, Kangawa K, Matsuo H. Cloning and sequence analysis of a cDNA encoding a precursor for rat C-type natriuretic peptide (CNP). FEBS Lett. 1990; 276: 209-213. **Ref.:** https://tinyurl.com/y8yjsyzx

3. Kojima Y, Tsukuda Y, Kawai Y, Tsukamoto A, Sugiura J, et al. Cloning, sequence analysis, and expression of ligninolytic phenoloxidase genes of the white-rot basidiomycete Coriolus hirsutus. J Biol Chem. 1990; 265: 15224-15230. **Ref.:** https://tinyurl.com/yagtu7xf

4. Chinkers M, Garbers DL, Chang MS, Lowe DG, Chin HM, et al. A membrane form of guanylate cyclase is an atrial natriuretic peptide receptor. Nature. 1989; 338: 78-83. **Ref.:** https://tinyurl.com/yd77zv7o

5. Koller KJ, Lowe DG, Bennett GL, Minamino N, Kangawa K, et al. Selective activation of the B natriuretic peptide receptor by C-type natriuretic peptide (CNP). Science. 1991; 252: 120-123. **Ref.:** https://tinyurl.com/yc522jkf

6. Stingo AJ, Clavell AL, Heublein DM, Wei CM, Pittelkow MR, et al. Presence of C-type natriuretic peptide in cultured human endothelial cells and plasma. Am J Physiol. 1992; 263: 1318-1321. **Ref.:** https://tinyurl.com/y9nc7txr

7. Kanai Y, Yasoda A, Mori KP, Watanabe-Takano H, Nagai-Okatani C, et al. Circulating osteocrin stimulates bone growth by limiting C-type natriuretic peptide clearance. J Clin Invest. 2017; 127: 4136-4147. **Ref.:** https://tinyurl.com/y9yncapr

8. Suga S, Nakao K, Kishimoto I, Hosoda K, Mukoyama M, et al. Phenotype-related alteration in expression of natriuretic peptide receptors in aortic smooth muscle cells. Circ Res. 1992; 71: 34-39. **Ref.:** https://tinyurl.com/y7pl6jl8

9. Brown J, Chen Q. Regional expression of natriuretic peptide receptors during the formation of arterial neointima in the rabbit. Circ Res. 1995; 77: 906-918. **Ref.:** https://tinyurl.com/yc66wk2t

10. Brown J, Zuo Z. Natriuretic peptide receptors in the fetal rat. Am J Physiol. 1995; 269: 253-268. https://tinyurl.com/y9q76ywq

11. Langub MC Jr, Dolgas CM, Watson RE Jr, Herman JP. The C-type natriuretic peptide receptor is the predominant natriuretic peptide receptor mRNA expressed in rat hypothalamus. J Neuroendocrinol. 1995; 7: 305-309. **Ref.:** https://tinyurl.com/y8ygfqzn

12. McArdle CA, Olcese J, Schmidt C, Poch A, Kratzmeier M, et al. C-type natriuretic peptide (CNP) in the pituitary: is CNP an autocrine regulator of gonadotropes? Endocrinology. 1994; 135: 2794-2801. **Ref.:** https://tinyurl.com/y8h32gzb

13. Doyle DD, Ambler SK, Upshaw-Earley J, Bastawrous A, Goings GE, et al. Type B atrial natriuretic peptide receptor in cardiac myocyte caveolae. Circ Res. 1997; 81: 86-91. **Ref.:** https://tinyurl.com/yaxu7ac6

14. Yasoda A, Komatsu Y, Nakao K, Ogawa Y. C-type natriuretic peptide(CNP)-A novel stimulator of bone growth formed through endochondral ossification. Nihon Rinsho. 2004; 62: 77-81. **Ref.:** https://tinyurl.com/y9cewjnu

15. Yasoda A, Komatsu Y, Chusho H, Miyazawa T, Ozasa A, et al. Overexpression of CNP in chondrocytes rescues achondroplasia through a MAPK-dependent pathway. Nat Med. 2004; 10: 80-86. **Ref.:** https://tinyurl.com/y96wrhwg

16. Bumpus FM, Pucell AG, Daud AI, Husain A. Angiotensin II: an intraovarian regulatory peptide. Am J Med Sci. 1988; 295: 406-408. **Ref.:** https://tinyurl.com/ycqqd9sp

17. Richards AM. The renin-angiotensin-aldosterone system and the cardiac natriuretic peptides. Heart. 1996; 76: 36-44. **Ref.:** https://tinyurl.com/y9r8bwaa

18. Vollmar AM, Mytzka C, Arendt RM, Schulz R. Atrial natriuretic peptide in bovine corpus luteum. Endocrinology. 1988; 123: 762-767. **Ref.:** https://tinyurl.com/ybytm8r9

19. Kim SH, Cho KW, Seul KH, Ryu H, Koh GY. Presence of immunoreactive atrial natriuretic peptide in follicular fluid, ovary and ovarian perfusates. Life Sci. 1989; 45: 1581-1589. **Ref.:** https://tinyurl.com/y9uftvaf

20. Kim SH, Cho KW, Lim SH, Hwang YH, Ryu H, et al. Presence and release of immunoreactive atrial natriuretic peptide in granulosa cells of the pig ovarian follicle. Regul Pept. 1992; 42: 153-162. **Ref.:** https://tinyurl.com/y7kmhtko

21. Pandey KN, Osteen KG, Inagami T. Specific receptor-mediated stimulation of progesterone secretion and cGMP accumulation by rat atrial natriuretic factor in cultured human granulosa-lutein (G-L) cells. Endocrinology. 1987; 121: 1195-1197. **Ref.:** https://tinyurl.com/yals9q49

22. Steegers EA, Hollanders JM, Jongsma HW, Hein PR. Atrial natriuretic peptide and progesterone in ovarian follicular fluid. Gynecol Obstet Invest. 1990; 29: 185-187. **Ref.:** https://tinyurl.com/ybpj6446

23. Musah AI, Bloch JF, Baker SL, Schrank GD. Human atrial natriuretic peptide infusion and ovarian venous progesterone secretion in Yucatan micropigs. J Reprod Fertil. 1994; 101: 109-113. **Ref.:** https://tinyurl.com/y7dvyvxo

24. Johnson KM, Hughes FM Jr, Fong YY, Mathur RS, Williamson HO, et al. Effects of atrial natriuretic peptide on rat ovarian granulosa cell steroidogenesis in vitro. Am J Reprod Immunol. 1994; 31: 163-168. **Ref.:** https://tinyurl.com/yaan4o3y

25. Kotani E, Usuki S, Kubo T. Effect of growth hormone releasing hormone on luteinizing hormone stimulated progestin biosynthesis in cultured rat ovarian granulosa cells. Gynecol Endocrinol. 1998; 12: 307-313. **Ref.:** https://tinyurl.com/y7av6fy5

26. Reith ME, Kim SS, Lajtha A. Binding sites for [3H] tetracaine in synaptosomal sodium channel preparations from mouse brain. Eur J Pharmacol. 1987; 143: 171-178. **Ref.:** https://tinyurl.com/y93lerfz

27. Piao FL, Park SH, Han JH, Cao C, Kim SZ, et al. Dendroaspis natriuretic peptide and its functions in pig ovarian granulosa cells. Regul Pept. 2004; 118: 193-198. **Ref.:** https://tinyurl.com/ybdfn2ya

28. Brunswig B, Budnik LT, Mukhopadhyay AK. Atrial natriuretic peptide-induced stimulation of cyclic GMP formation by isolated bovine luteal cells. J Reprod Fertil. 1989; 86: 665-669. **Ref.:** https://tinyurl.com/y7x66drg

29. Jankowski M, Reis AM, Mukaddam-Daher S, Dam TV, Farookhi R, et al. C-type natriuretic peptide and the guanylyl cyclase receptors in the rat ovary are modulated by the estrous cycle. Biol Reprod. 1997; 56: 59-66. **Ref.:** https://tinyurl.com/ycb6drkz

30. Benfenati F, Cimino M, Agnati LF, Fuxe K. Quantitative autoradiography of central neurotransmitter receptors: methodological and statistical aspects with special reference to computer-assisted image analysis. Acta Physiol Scand. 1986; 128: 129-146. **Ref.:** https://tinyurl.com/ychmcvgt

31. Munson PJ, Rodbard D. Ligand: A versatile computerized approach for characterization of ligand-binding systems. Anal Biochem. 1980; 107: 220-239. **Ref.:** https://tinyurl.com/ybj89aoq

32. Cho KW, Seul KH, Kim SH, Seul KM, Koh GY. Atrial pressure, distension, and pacing frequency in ANP secretion in isolated perfused rabbit atria. Am J Physiol. 1991; 260: 39-46. **Ref.:** https://tinyurl.com/y9qeg7q9

33. Joseph LJ, Desai KB, Mehta MN, Mathiyarasu R. Measurement of specific activity of radiolabelled antigens by a simple radioimmunoassay technique. Int J Rad Appl Instrum B. 1988; 15: 589-590. **Ref.:** https://tinyurl.com/ychgxppc

34. Schulz S, Singh S, Bellet RA, Singh G, Tubb DJ, et al. The primary structure of a plasma membrane guanylate cyclase demonstrates diversity within this new receptor family. Cell. 1989; 58: 1155-1162. **Ref.:** https://tinyurl.com/ybjosdok

35. Kim SH, Cho KW, Oh SH, Hwang YH, Lim SH, et al. Immunoreactive atrial natriuretic peptides in the oocyte. Comp Biochem Physiol Comp Physiol. 1993; 104: 219-223. **Ref.:** https://tinyurl.com/ya6nradz

36. Tornell J, Carlsson B, Billig H. Atrial natriuretic peptide inhibits spontaneous rat oocyte maturation. Endocrinology. 1990; 126: 1504-1508. **Ref.:** https://tinyurl.com/ycx8ykmc

37. Porter JG, Wang Y, Schwartz K, Arfsten A, Loffredo A, et al. Characterization of the atrial natriuretic peptide clearance receptor using a vaccinia virus expression vector. J Biol Chem. 1988; 263: 18827-18833. **Ref.:** https://tinyurl.com/yc6kgyyj

38. Maack T, Suzuki M, Almeida FA, Nussenzveig D, Scarborough RM, et al. Physiological role of silent receptors of atrial natriuretic factor. Science. 1987; 238: 675-678. **Ref.:** https://tinyurl.com/y97c5m5f

39. Schenk DB, Phelps MN, Porter JG, Fuller F, Cordell B, et al. Purification and subunit composition of atrial natriuretic peptide receptor. Proc Natl Acad Sci USA. 1987; 84: 1521-1525. **Ref.:** https://tinyurl.com/y8xd4a62

40. Leitman DC, Andresen JW, Catalano RM, Waldman SA, Tuan JJ, et al. Atrial natriuretic peptide binding, cross-linking, and stimulation of cyclic GMP accumulation and particulate guanylate cyclase activity in cultured cells. J Biol Chem. 1988; 263: 3720-3728. **Ref.:** https://tinyurl.com/ya7w3zs9

41. Thibault G, Grove KL, Deschepper CF. Reduced affinity of iodinated forms of Tyr0 C-type natriuretic peptide for rat natriuretic peptide receptor B. Mol Pharmacol. 1995; 48: 1046-1053. **Ref.:** https://tinyurl.com/ybkqvey4

42. Morishita Y, Sano T, Kase H, Yamada K, Inagami T, et al. HS-142-1, a novel nonpeptide atrial natriuretic peptide (ANP) antagonist, blocks ANP-induced renal responses through a specific interaction with guanylyl cyclase-linked receptors. Eur J Pharmacol. 1992; 225: 203-207. **Ref.:** https://tinyurl.com/y8aen42e

43. Morishita Y, Matsuda Y. HS-142-1; a novel polysaccharide, specifically recognizes guanylyl cyclase-containing ANP receptor. Tanpakushitsu Kakusan Koso. 1993; 38: 903-908. **Ref.:** https://tinyurl.com/y8ebbz2b